

## Effects of torsional vibration of a propulsion shafting system using a large-scale two stroke marine engine with a waste heat recovery system

Yang-Gon Kim<sup>1</sup> · Kwon-Hae Cho<sup>2</sup> · Ue-Kan Kim<sup>†</sup>

(Received February 9, 2017 ; Revised March 28, 2017 ; Accepted April 17, 2017)

**Abstract:** Many marine vessels recently built are equipped with ultra-long stroke engines with high propulsion efficiency, and an engine de-rating technology and tuning technology are applied to comply with the more stringent environmental regulations and to reduce fuel consumption. Waste heat recovery systems (hereafter WHRSs) recover the waste heat from the exhaust gas emitted by the ship and use it in motor power for propulsion or in generators to supply electric power to the ship. In this case, it can be expected that the fuel consumption rate will be improved at the same speed, depending on the required horsepower reduction effect. However, this is accompanied by a tendency of increased torsional vibration excitation forces in the operating range of this system, compared to the standard engine without a WHRS.

In this paper, the performance and the dynamic characteristics of a marine diesel engine, with application of a waste heat system, are reviewed, and the effects on the torsional vibration of a corresponding propulsion shafting system, in an ultra large container vessel equipped with the corresponding system, are studied.

**Keywords:** Waste heat recovery system (WHRs), Torsional vibration, Propulsion shafting system

### 1. Introduction

The international maritime industry is facing serious economic difficulties owing to the over-supply of vessels and the impact of high oil prices, as well as the International Maritime Organization's stringent measures to reduce greenhouse gas emissions from vessels. Various fuel saving measures have been developed and implemented to address this issues. Measures include slow steaming, trim and draft optimization, navigation route optimization, hull and propeller grinding, air lubrication, a combination of a super-long-stroke engine and a low-speed larger-diameter propeller, engine tuning technologies, and waste heat recovery systems (WHRs). Among them, the WHRS recovers heat energy from the exhaust gas discharged from the marine engine and using steam turbine and gas turbines, and applies this energy for propulsion or in an electric generating plant for the ship.

WHRs have been studied for both land-based and marine applications. Bonilla *et al.* [1] discuss waste heat recovery technologies to utilize waste heat from industrial complexes in

the Basque region of Spain. Nguyen *et al.* [2] discuss the use of a steam Rankine cycle, an organic Rankine cycle and a Kalina cycle to produce power from low temperature waste heat sources up to 250 °C. Al-Rabghi *et al.* [3] review a WHRS for power generation and process heating in the oil and gas industry. Singh *et al.* [4] discuss waste heat recovery techniques that can be utilized in marine applications. Dzida *et al.* [4]-[6] report that, for a 9RTA96C engine mounted on a large container ship, fuel consumption can be reduced by approximately 10% using a combination of gas and steam turbines. The output also can be increased by approximately 11% through recovery of the exhaust gas heat energy without changing the engine output. In addition, with the same WHRS, the fuel consumption can be further reduced by 6.9-14.6%, relative to the conventional system, when the gas turbine is situated downstream of the turbocharger. Sencic *et al.* [7] studied the effect of these factors on the overall efficiency of the combined power plant, by adjusting the fuel injection timing and exhaust valve opening and closing timing for the 6S50MC engine. They reported that

† Corresponding Author (ORCID: <https://orcid.org/0000-0002-9662-2175>): Division of Mechanical Systems Engineering, Korea Maritime and Ocean University, 727, Taejong-ro, Yeongdo-gu, Busan 49112, Korea, E-mail: [nvh@kmou.ac.kr](mailto:nvh@kmou.ac.kr), Tel: 051-410-4361

1 Korean Register, E-mail: [ygkim@krs.co.kr](mailto:ygkim@krs.co.kr), Tel: 070-8799-8273

2 Department of Offshore Plant Management, Korea Maritime and Ocean University, E-mail: [khcho@kmou.ac.kr](mailto:khcho@kmou.ac.kr), Tel: 051-410-4250

This is an Open Access article distributed under the terms of the Creative Commons Attribution Non-Commercial License (<http://creativecommons.org/licenses/by-nc/3.0>), which permits unrestricted non-commercial use, distribution, and reproduction in any medium, provided the original work is properly cited.

the efficiency could be maximized by advancing both the fuel injection timing and the exhaust valve opening. However, this requires more fuel to be injected, resulting in a decrease in engine efficiency. Landeka *et al.* [8] reported that the efficiency can be further improved, by 2.2 -4%, by the addition of a turbocharger, with a multi-stage compression system, to marine engines at 100% load, using a WHRS. On the other hand, when the engine load is over 80%, the scavenge air pressure may exceed the maximum allowable range. Therefore, the exhaust gas bypass valve must be adjusted so that excess exhaust gas can flow into the gas turbine. In this manner, a WHRS can improve the fuel consumption and reduce the amount of CO<sub>2</sub> and NO<sub>x</sub> generated, but adjustment of the engine parameters to improve the overall efficiency of the system tends to increase the torsional vibration excitation force from the marine engine.

In this paper, the performance of a marine diesel engine and characteristics of the excitation forces, in relation to the torsional vibration of the propulsion shafting system, are compared and analyzed when WHRS is installed. In addition, the dynamic characteristics of the torsional vibration of a propulsion shafting system, equipped with a 7G80ME-C9.5 engine, are investigated by applying a WHRS, optimized for the operating conditions of a post Panamax-class container ship.

## 2. Engine performance and characteristics of torsional exciting force in shafting system according to waste heat recovery system

Generally, the waste heat of exhaust gases from a marine engine is recovered through a turbocharger and an exhaust gas economizer. The turbocharger drives a turbine and compressor by using exhaust gas waste heat. Therefore, it provides excess scavenge air to the cylinder for combustion to improve the output and thermal efficiency of the engine. To date, marine diesel engines have reached up to 50% thermal efficiency owing to continued technological advances, which is significantly higher than that of other gas or steam turbines. Despite these efforts, waste heats from a ship is approximately 50%, of which waste heat in exhaust gases (25.5%) is the largest percentage [9]. Therefore, a WHRS has been developed for recovering the waste heat from the exhaust gas from marine engines [9]-[11].

Figure 1 shows a conceptual diagram of an installed WHRS. As shown in this figure, most of the exhaust gas from the engine generates low and high pressure steam through the

exhaust gas boiler with double steam pressure vessels; the steam turbine is driven by the high-pressure steam. On the other hand, some exhaust gases (up to 11%) bypassing the turbocharger drive the gas turbine. Here, the steam and the gas turbines are connected to the generator through a clutch, the electricity produced is supplied to the propulsion motor, and consequently, the output of the main engine is reduced. However, to increase the efficiency of this system, it is necessary to properly adjust the engine performance for this system so that the temperature of the exhaust gas is higher than that of the existing engine.

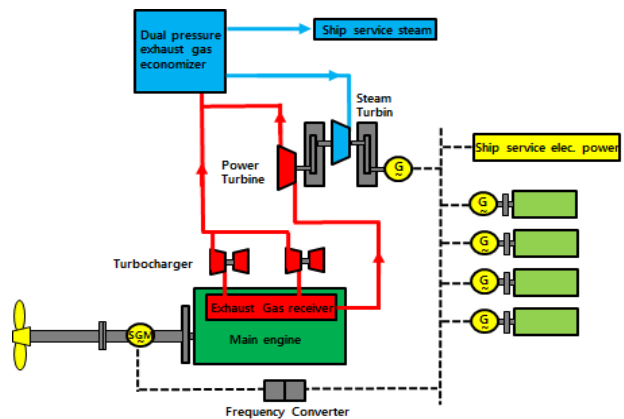
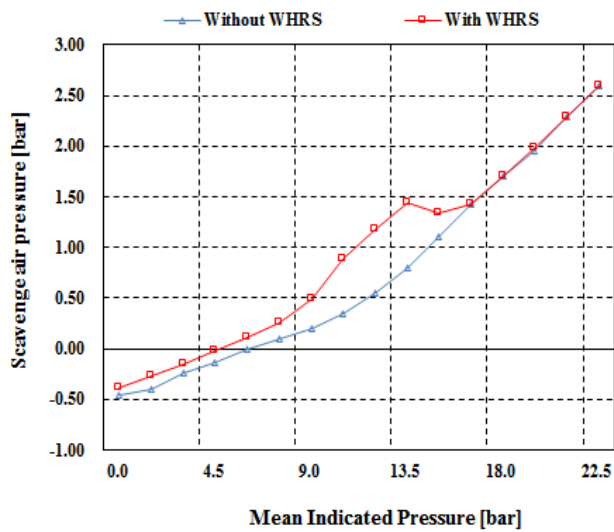


Figure 1: Design concept of waste heat recovery system

Table 1 gives the specifications of the marine engine on the ship to which WHRS is applied. To increase the efficiency of the WHRS, the fuel injection timing and the exhaust valve opening and closing timing were advanced so that more fuel could be injected. Figure 2 ~ Figure 5 compare the performance of the engine before and after applying the WHRS using the CEAS engine calculation program [12][13]. As shown in these figures, as the system is applied, the scavenge air pressure and compression pressure increase to 0.6 bar and 37.3 bar, respectively, in the range of the mean effective pressure at which the exhaust gas bypass valve is closed, i.e., less than 13.5 bar. In addition, the fuel injection amount is more than 2g/kWh higher than the conventional setting value. As a result, it can also be seen that the maximum temperature increase of the exhaust gas is 49.3°C, at an engine load of 85%. This system opens the exhaust gas bypass valve at an average effective pressure greater than 13.5 bar, allowing up to 11% of the total exhaust to flow directly into the gas turbine without going through the turbocharger. Accordingly, both the scavenging and the compression pressures are significantly reduced in the region where the average effective pressure is 13.5 bar or greater.

**Table 1:** Specifications for main engine

Items	Detail
Type	7G80ME-C9.5
SMCR (kW x rpm)	28,660 x 68.6
Cylinder bore (mm)	800
Stroke (mm)	3,720
MEP (bar)	19.2
Model of turbocharger	ABB A175-L
Number of turbocharger	2 sets



**Figure 2:** Comparison of scavenge air pressure in 7G80ME-C9.5 engine with/without waste heat recovery system

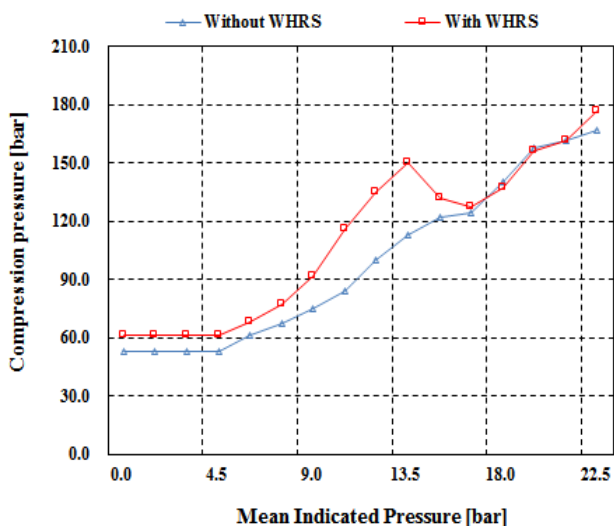


**Figure 3:** Comparison of compression pressure in 7G80ME-C9.5 engine with/without waste heat recovery system

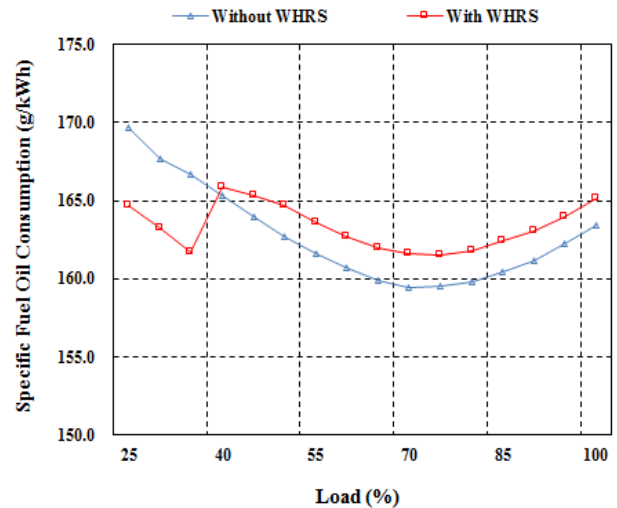


**Figure 4:** Comparison of fuel consumption rate in 7G80ME-C9.5 engine with/without waste heat recovery system

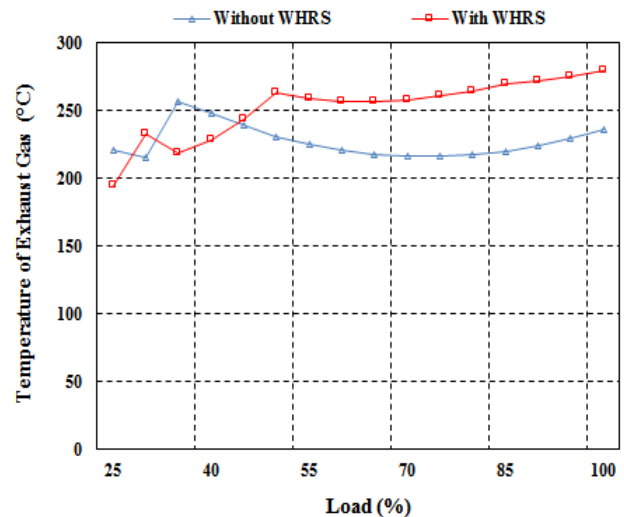


**Figure 5:** Comparison of exhaust gas temperature in 7G80ME-C9.5 engine with/without waste heat recovery system

**Figure 6** and **Figure 7** show the characteristics of the torsional excitation force in the shafting system, according to the simulated results from the application of the WHRS to the marine engine described in **Table 1** [14][15]. As can be seen in these figures, adjusting engine parameters to increase the efficiency of the WHRS causes an increase in both the scavenge air pressure and the compression pressure, and this increases the torsional vibratory torque by more than 20%, within the range of the mean indicated pressure, below 13.5 bar, where the exhaust gas bypass valve is closed.

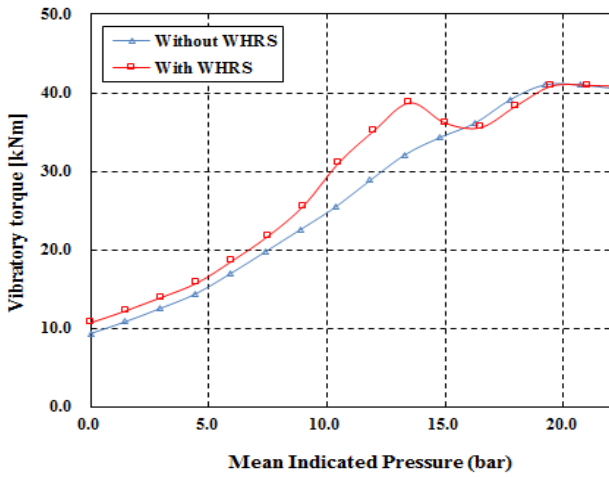


**Figure 6:** Comparison of 7th order vibratory torque in 7G80ME-C9.5 engine with/without waste heat recovery system

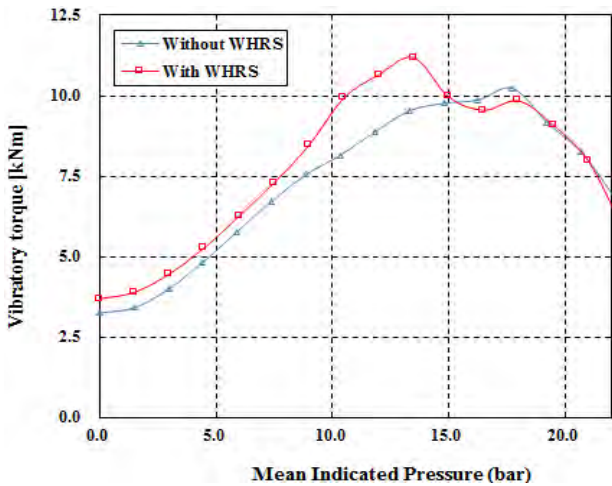


**Figure 7:** Comparison of 11th order vibratory torque in 7G80ME-C9.5 engine with/without waste heat recovery system

### 3. Effect of torsional vibration for propulsion shafting system according to the application of waste heat recovery system

In this section, the characteristic effects of torsional vibration in the propulsion shafting system of a ship are investigated. A WHRS developed to improve fuel consumption rate is applied to the ship, which is a post Panamax class container ship equipped with a marine engine, as described in **Table 1**. A gas and a steam turbines are used in combination to recover the heat of the exhaust gas. In addition, an electric motor is attached to the intermediate shaft to utilize the electricity generated from the recovered waste heat source as propulsion power.

#### 3.1 Modeling of propulsion shafting system

As the propulsion shaft system is a highly complex vibration system, it is difficult to analyze it directly. Therefore, the

torsional vibration of the corresponding system should be interpreted by replacing the mass inertia moment and the torsional stiffness coefficient with numerous disks, mechanically equivalent circular shafts, and uniform diameter circular rods without mass. **Table 2** and **Table 3** present the specifications of the ship's shafting system and the viscous-spring dampers selected by the shafting designer of the ship. **Figure 8** shows the results of the equivalent model of the propulsion shafting system attached with the viscous-spring dampers described in **Table 3**.

**Table 2:** Specifications for the shafting system

Items		Detail
Main Engine	Type	7G80ME-C9.5
	MCR (kW x rpm)	28,660 x 68.6
	Cylinder bore (mm)	800
	Stroke (mm)	3,720
	MEP (bar)	21
	Ratio of connecting rod	0.5
	Reciprocating mass (N/cylinder)	138,872
	Firing order	1-7-2-5-4-3-6
	Moment of inertia of flywheel (kgm <sup>2</sup> )	60,000
Shaft	Diameter of no.1 intermediate shaft (mm)	850
	Diameter of no.2 intermediate shaft (mm)	850
	Diameter of no.3 intermediate shaft (mm)	850
	Diameter of propeller shaft (mm)	865
Shaft Generator & Motor	Output (kW)	2,000
	Diameter of rotor shaft (mm)	850
Propeller	Type	FPP
	Number of blade	4
	Diameter (m)	10.2
	Moment of inertia in water (kgm <sup>2</sup> )	359,813

**Table 3:** Specifications for torsional vibration damper

Items	Detail
Type	D350/2/V/M
Outer inertia / Inner inertia (kgm <sup>2</sup> )	30,200 / 1,810
Stiffness (MNm/rad)	154.99
Relative damping (Nms/rad)	450,000
Permissible vibratory torque at continuous operation (kNm)	1,470
Permissible vibratory torque at continuous operation (kNm)	2,210
Permissible thermal load (kW)	200

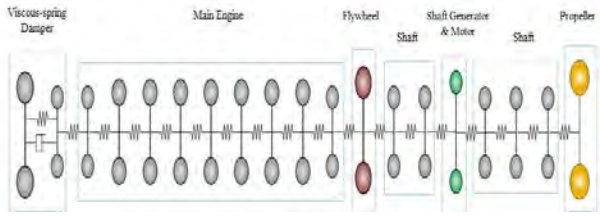


**Figure 8:** Multi-degree modeling of the propulsion shafting system in the example ship with waste heat recovery system

### 3.2 Exciting torque by gas pressure and inertia force

The rotational moment due to the combustion gas pressure in the cylinder, and the reciprocating mass inertia force, act on the crankshaft of a marine engine. As they constantly fluctuate with a constant period, the rotational moment of the crank throw becomes irregular. As shown in **Figure 9**, the gas pressure acting on the top of the piston turns the crank through the connecting rod, and the tangential force  $F_t$  becomes the effective force for rotating the crankshaft. The crank rotational moment ( $M_g(\theta)$ ) due to the gas pressure, and the rotational moment due to the reciprocating mass ( $m_{rec}$ ) on the piston and the connecting rod are calculated in **Equations (1)** and **Equation (2)**, respectively [16]-[20]. Here,  $L$  is the length of the connecting rod,  $r$  is the crank radius,  $\lambda$  is the connecting rod ratio, and  $\omega$  is the rotational angular velocity of the crankshaft.

$$M_g(\theta) = P_g r \left( \sin \theta + \frac{\lambda}{2} \sin 2\theta \right) \tag{1}$$

$$M_r(\theta) = m_{rev} \omega^2 r^2 \left( \frac{\lambda}{4} \sin \theta - \frac{1}{2} \sin 2\theta - \frac{3\lambda}{4} \sin 3\theta - \frac{\lambda^2}{4} \sin 4\theta - \dots \right) \tag{2}$$

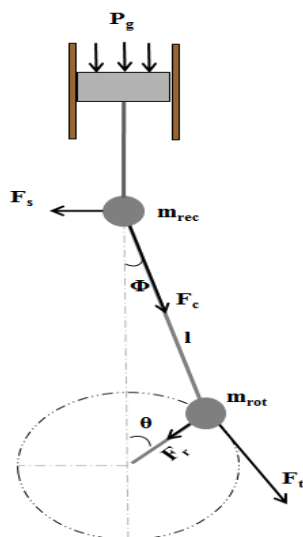


**Figure 9:** Tangential force of crankshaft

### 3.3 Torsional forced vibration analysis by Transfer matrix method

method

The mode analysis method, the mechanical impedance method, and the transfer matrix method, are all used in torsional forced vibration analyses of shafting systems with multiple degrees of freedom. In this study, the transfer matrix method is used, as it is more efficient, in terms of calculation time. The forced vibration equation of the shafting system can be expressed as the matrix in **Equation (3)** [16]-[20]. Here,  $[J]$ ,  $[C]$ , and  $[K]$  are the mass moment of the inertia matrix, the damping coefficient matrix, and the stiffness coefficient matrix, respectively.  $\{Q(t)\}$  is a vector representing the exciting force.

$$[J]\{\ddot{\theta}\} + [C]\{\dot{\theta}\} + [K]\{\theta\} = \{Q(\theta)\} \tag{3}$$

The method of interpreting the steady response due to the forced vibration by use of the transfer matrix method [12]-[16] is now described. The torque between  $J_{i-1}$  and  $J_i$ , and the torsional angle  $\theta$  between two mass points in the torsional vibration system, as shown in **Figure 10**, are given by **Equation (4)**. Here,  $L$  is the left side of the mass moment of inertia,  $R$  is the right side of the mass moment of inertia,  $T$  is the internal torque,  $\theta$  is the displacement,  $J$  is the mass moment of inertia,  $c$  is the damping coefficient,  $k$  is the torsional stiffness coefficient, and  $\omega$  is the rotational angular velocity.

$$\begin{aligned} T_j^L &= T_{j-1}^F \\ \theta_j^L &= \theta_{j-1}^R + \frac{T_{j-1}^R}{k_j + j\omega c_j} \end{aligned} \tag{4}$$

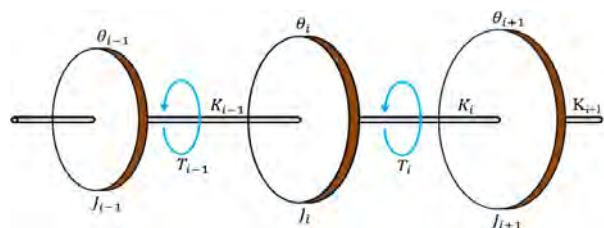


**Figure 10:** Multi-degree of torsional vibration system

As the solution of the forced damped vibration has the form of a complex number, it is divided into a real part and an imaginary part and becomes an expanded field matrix, as shown in **Equation (5)**. Here, the superscript (r) is the real part and (i) is the imaginary part.

$$\{z\}_j^L = [F]\{z\}_{j-1}^R \tag{5}$$

$$\begin{bmatrix} \theta_j^L \\ \tau_j^L \\ \theta_j^R \\ \tau_j^R \\ 1 \end{bmatrix} = \begin{bmatrix} 1 & \frac{k_{j-1}}{k_{j-1}^2 + c_{j-1}^2 \omega^2} & 0 & \frac{c_{j-1} \omega}{k_{j-1}^2 + c_{j-1}^2 \omega^2} & 0 \\ 0 & 1 & 0 & 0 & 0 \\ 0 & \frac{-c_{j-1} \omega}{k_{j-1}^2 + c_{j-1}^2 \omega^2} & 1 & \frac{k_{j-1}}{k_{j-1}^2 + c_{j-1}^2 \omega^2} & 0 \\ 0 & 0 & 0 & 1 & 0 \\ 0 & 0 & 0 & 0 & 1 \end{bmatrix} \begin{bmatrix} \theta_{j-1}^L \\ \tau_{j-1}^L \\ \theta_{j-1}^R \\ \tau_{j-1}^R \\ 1 \end{bmatrix}$$

Assuming that the sinusoidal torque acts on the i-th material point, the displacement and torque of the material point on the left and right sides are given by **Equation (6)**.

$$\begin{aligned} \tau_j^R + \rho_j(t) &= \tau_j^L + (-\omega^2 J_j + j\omega c_j + k_j) \theta_j^L \\ \theta_j^L &= \theta_j^R \end{aligned} \tag{6}$$

This equation is divided into a real part and an imaginary part, as in the previous case and becomes an extended point matrix, as shown in **Equation (7)**.

$$\begin{bmatrix} \theta_j^R \\ \tau_j^R \\ \theta_j^L \\ \tau_j^L \\ 1 \end{bmatrix} = \begin{bmatrix} 1 & 0 & 0 & 0 & 0 \\ -\omega^2 J + k & 1 & \omega c & 0 & -\rho(t) \\ 0 & 0 & 1 & 0 & 0 \\ \omega c & 1 & -\omega^2 J + k & 1 & -\rho(t) \\ 0 & 0 & 0 & 0 & 1 \end{bmatrix} \begin{bmatrix} \theta_{j-1}^R \\ \tau_{j-1}^R \\ \theta_{j-1}^L \\ \tau_{j-1}^L \\ 1 \end{bmatrix} \tag{7}$$

The relationship between the state vector on the right side of the i-point, and the state vector on the right-hand side of the i-1 point is delineated in **Equation (8)**.

$$\{z\}_j^R = [P][F_{i-1}]\{z\}_{j-1}^R \tag{8}$$

Here, [Pi] is a point matrix of i-material points, and [Fi-1] is a field matrix between i and i-1 material points. Therefore, the transfer matrix of the entire shafting system is the product of the field matrix between each material point and the point matrix of each material point, as shown in **Equation (8)**. By interpreting the boundary condition at each end of the state vector, it is then possible to analyze the torsional forced vibration amplitude, and the vibration torque for each mass point of the propulsion shafting system.

### 3.4 Result and consideration of torsional forced vibration analysis by transfer matrix method

The torsional forced vibration of the propulsion shafting system in **Figure 8** was analyzed using the transfer matrix

method. **Figure 11** compares the additional torsional stresses acting on the crankshaft depending on the application of the WHRS, to the viscous-spring dampers mounted on the propulsion shafting system of the ship. Here,  $\tau_{cs1}$  is the fatigue limit value of the crankshaft, determined according to IACS UR M53 and the guidelines of the engine manufacturer, with  $\tau_{cs2}$  as the limit for the yield strength [21][22]. As shown in **Figure 11**, the additional torsional stress on the crankshaft increases by (8.5 and 3.8-11.5) % in the range of 25rpm and 39-59rpm, respectively, when the waste heat recovery system is applied. As can be seen, the additional torsional stress acting on the crankshaft is slightly above the fatigue limit value (27 N/mm<sup>2</sup>) at 25 rpm. Therefore, when the waste heat recovery system is operated, it exceeds the fatigue limit at 25 rpm, and thus the barred speed range should be set to prevent fatigue fracture that may occur within the ship's life (20-25years).

**Figure 12** shows the additional torsional stresses in the crankshaft when no.5 cylinder misfires. Here, the misfiring condition means that there is no injection, but there is compression [23]. As seen in this figure, the additional torsional stress on the crankshaft increases by (8.2 and 11.8-36.7) % in the range of 25rpm and 39-59rpm, respectively.

**Figure 13 ~ Figure 16** show the additional torsional stresses in the intermediate and propeller shafts under normal-firing and no.5 cylinder misfiring conditions. Here,  $\tau_{is1}$  is the fatigue limit value of the intermediate shaft, determined according to IACS UR M68, and with  $\tau_{is2}$  as the limit for the yield strength [23]. The fatigue limit value of the propeller shaft,  $\tau_{ps1}$ , is determined according to the same criterion, and  $\tau_{ps2}$  is the limit for the yield strength [23]. As shown in these figures, as the WHRS is applied, the additional torsional stress in the intermediate shaft and propeller shaft under normal firing conditions, increase by (8.5 and 8.4) %, respectively, at 25 rpm. In addition, it was found that the additional torsional stress in each shaft, under no.1 cylinder misfiring conditions, increased by (8.0 and 7.8) %, respectively. The torsional stress increased sharply by up to (42.9 and 41.8 %) in each shaft in the range of 40 to 60 rpm. In particular, as it exceeds the fatigue limit value of 57 rpm for the propeller shaft, it was necessary to set the barred speed range to avoid fatigue fractures of the shaft during the vessel's life time, which is 20-25 years.

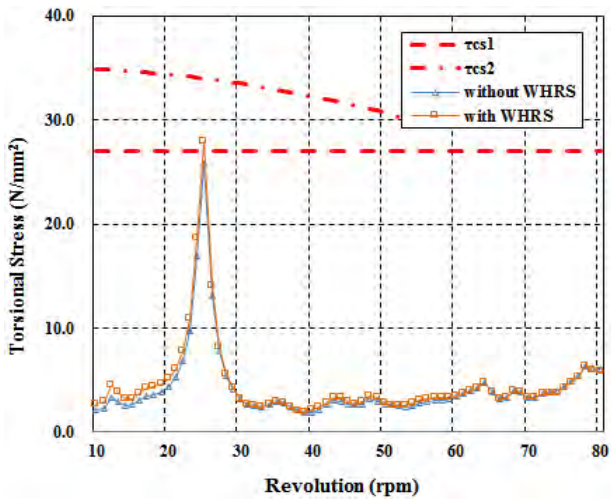


Figure 11: Comparison of synthesized torsional stress in no.7 crank throw at normal firing condition with/without WHRS

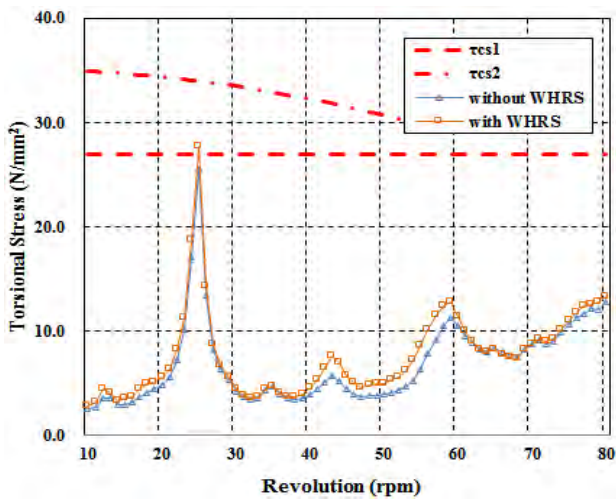


Figure 12: Comparison of synthesized torsional stress in no.7 crank throw at no.5 cylinder misfiring condition with/without WHRS

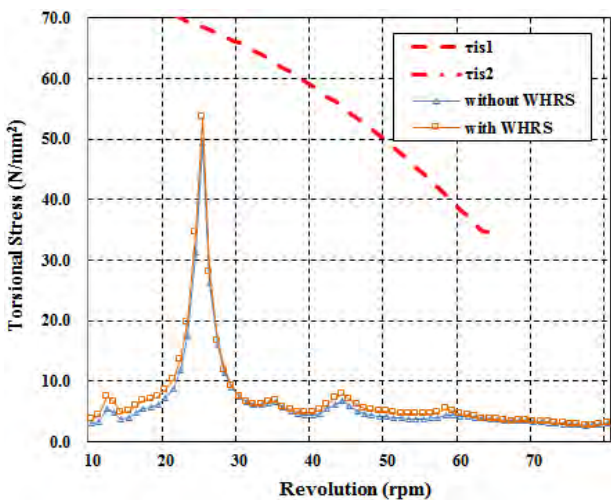


Figure 13: Comparison of synthesized torsional stress in no.7 crank throw at normal firing condition with/without WHRS

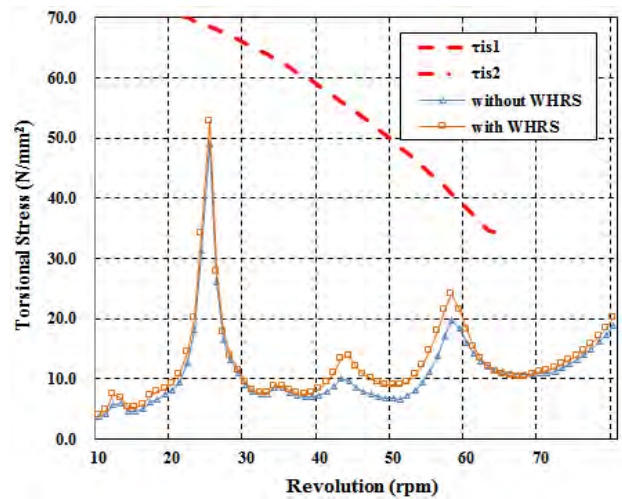


Figure 14: Comparison of synthesized torsional stress in no.3 intermediate shaft at no.5 cylinder misfiring condition with/without WHRS

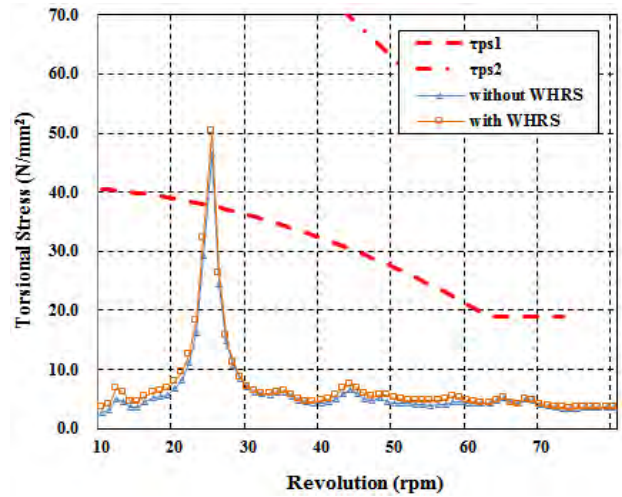


Figure 15: Comparison of synthesized torsional stress in propeller shaft at normal firing condition with/without WHRS

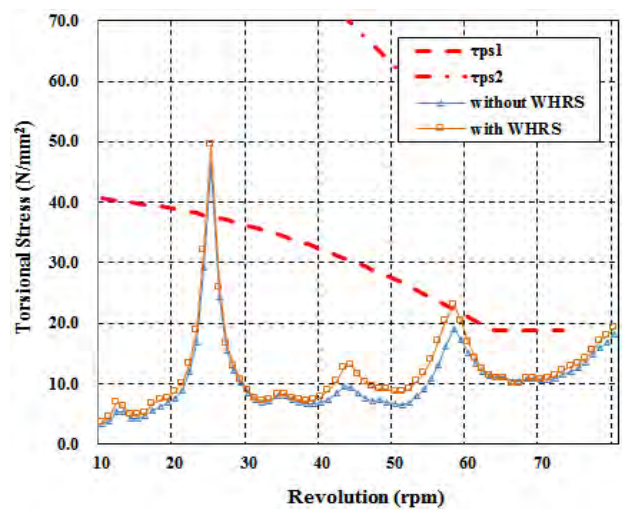


Figure 16: Comparison of synthesized torsional stress in propeller shaft at no.5 cylinder misfiring condition with/without WHRS

#### 4. Conclusions

In this study, the performance of the main engine and characteristics of the excitation forces causing torsional vibration were compared and reviewed. This was in relation to the application of a WHRS intended to improve fuel consumption. The effects of the dynamic characteristics of the torsional vibration of the propulsion shafting system caused by corresponding systems were examined. The results of this study are summarized as follows.

(1) With the application of the WHRS developed for recovering the waste heat from the exhaust gas discharged from a marine engine, it was necessary to adjust the parameters of the existing standard engine to increase the efficiency of the system. Specifically, the fuel injection timing and the exhaust valve opening and closing timing were advanced, and the fuel injected in the cylinder was approximately 2 g/kWh more. As a result, it could be seen that the temperature of the exhaust gas discharged from the engine increased up to 49.3°C at an engine load of 85%. However, this increased the scavenge air pressure and compression pressure. Therefore, it was found that the torsional vibratory torque was increased by more than 20% in the range where the exhaust gas bypass valve was closed (below an average effective pressure of 13.5 bar).

(2) When the WHRS was installed, the additional torsional stress on the crankshaft increased by (8.5 and 3.8-11.5) %, respectively, under normal firing conditions, and increased by (8.2 and 11.8-36.7) %, respectively, when no.5 cylinder misfired, at 24 rpm and 39-59 rpm respectively. The additional torsional stress on the crankshaft exceeded the fatigue limit at 25 rpm; therefore, a barred speed range should be set to prevent fatigue fracture that could occur within the ship's life time of 20-25 years.

(3) In the case of the intermediate and propeller shafts, the additional torsional stress applied to each shaft was increased in a manner similar to that of the crankshaft. However, in the case of the propeller shaft, as it exceeded the fatigue limit of the corresponding shaft, determined according to IACS UR M68, at 57 rpm when no.5 cylinder misfired, it was necessary to set the barred speed range additionally. However, this requires further study, as there may be differences, depending on the propulsion shafting system to which this system is applied.

#### References

- [1] J. J. Bonilla, J.M. Blanco, I. Lopez, and J. M. Sala, "Technological recovery potential of waste heat in the industry of the Basque country," *Applied Thermal Engineering*, vol. 17, no. 3, pp. 283-288, 1997.
- [2] T. Q. Nguyen, J. D. Slawnwhite, and K. G. Boulama, "Power generation from residual industrial heat," *Energy Conversion and Management*, vol. 51, no. 11, pp. 2220-2229, 2010.
- [3] M. Al-rabghi, M. Beirutty, M. Akyurt, Y. Najjar, and T. Alp, "Recovery and utilization of waste heat," *Heat Recovery Systems and CHP*, vol. 13, no. 5, pp. 463-470, 1993.
- [4] N. Dzida, *Possible Efficiency Increasing of Ship Propulsion and Maritime Power Plant with the System Combined of Marine Diesel Engine, Gas Turbine and Steam Turbine*, *Advances in Gas Turbine Technology*, Chapter 3, Gdansk University of Technology, Gdansk, Poland, 2011.
- [5] M. Dzida and J. Mucharski, "On the possible increasing of efficiency of ship power plant with the system combined of marine diesel engine, gas turbine and steam turbine in case of main engine cooperation with the gas turbine fed in parallel and the steam turbine," *Polish Maritime Research*, vol. 16, no. 2, pp. 40-44, 2009.
- [6] M. Dzida, J. Girtler, and S. Dzida, "On the possible increasing of efficiency of ship power plant with the system combined of marine diesel engine, gas turbine and steam turbine in case of main engine cooperation with the gas turbine fed in series and the steam turbine," *Polish Maritime Research*, vol. 16, no. 3, pp. 40-44, 2009.
- [7] T. Sencic, N. Racic, and B. Frankovic, "Influence of low-speed marine diesel engine settings on waste heat availability," *Brodogradnja: Faculty of Mechanical Engineering and Naval Architecture*, vol. 63, no. 4, pp. 329-335, 2012.
- [8] P. Landeka and G. Radica, "Efficiency increase in ship's primal energy system using a multistage compression with intercooling," *Thermal Science*, vol. 20, no. 2, pp. 1399-1406, 2016.
- [9] MAN Diesel & Turbo, *Waste Heat Recovery System (WHRS) for Reduction of Fuel Consumption, Emissions and EEDI*, Copenhagen, Denmark, 2012.
- [10] E. Shinichiro, M. Takahiro, and I. Yoshihiro, "Ship propulsion/electric power hybrid system recovering waste heat of marine diesel engines," *Mitsubishi Heavy*

Industries Technical Review, vol. 50, no. 3, pp. 54-58, 2013.

- [11] Yoshihiro, S. Keiichi, K. Takayuki, O. Yoshihisa, and O. Yuji, "Development of super waste-heat recovery system for marine diesel engines," *Misubishi Heavy Industries Review*, vol. 48, no. 1, pp. 17-21, 2011.
- [12] MAN Diesel & Turbo, *CEAS Engine Data Report: 7G80ME-C9.5 with High Load Tuning*, Copenhagen, Denmark, 2016.
- [13] MAN Diesel & Turbo, *Performance Data-WHRS no.35111-2015*, MAN Diesel & Turbo, Copenhagen, Denmark, 2015.
- [14] MAN Diesel & Turbo, *Harmonic Analysis of Tangential Pressure no. 249987*, MAN Diesel & Turbo, Copenhagen, Denmark, 2016.
- [15] MAN Diesel & Turbo, *Harmonic Analysis of Tangential Pressure no. 249725*, MAN Diesel & Turbo, Copenhagen, Denmark, 2015.
- [16] Korean Register, *Control of Ship Vibration and Noise*, Third edition, Textbook Publisher, Korea, 2012 (in Korean).
- [17] H. J. Jeon and U. K. Kim, *Machine Dynamics*, Hyo-sung publisher, Korea, 1999 (in Korean).
- [18] H. J. Jeon and D. C. Lee, *Vibration of Propulsion Shafting*, Dasom publisher, Korea, 2003 (in Korean).
- [19] W. K. Wilson, *Practical Solution of Torsional Vibration Problems*, vol. 1-5, Chapman & Hall, London, United Kingdom, 1942.
- [20] E. J. Nestorides, B.I.C.E.R.A. (The British International Combustion Engine Research Association), *Handbook of Torsional Vibration*, Cambridge University Press, London, United Kingdom, 1958.
- [21] MAN Diesel & Turbo, *Limits for Torsional Stress in Crankshafts, Operated in Transient Condition*, Sheet no.242681, MAN Diesel & Turbo, Copenhagen, Denmark, 1997.
- [22] IACS, M53: *Calculation of Crankshafts for I.C. Engines*, International Association of Classification Societies Ltd., London, United Kingdom, 2011.
- [23] IACS, M68: *Dimension of Propulsion Shafts and Their Permissible Torsional Vibration Stresses*, International Association of Classification Societies Ltd., London, United Kingdom, 2015.